Published in final edited form as:
Mitochondrion. 2014 July ; 17: 132–140. doi:10.1016/j.mito.2014.04.008.

ERK-mediated phosphorylation of TFAM downregulates mitochondrial transcription: Implications for Parkinson's disease

Kent Z.Q. Wang[1], **Jianhui Zhu**[1], **Ruben K. Dagda**[1,†], **Guy Uechi**[2], **Salvatore J. Cherra III**[1,†], **Aaron M. Gusdon**[1,†], **Manimalha Balasubramani**[2], and **Charleen T. Chu**[1,3,4,*]

[1]Department of Pathology, Division of Neuropathology, University of Pittsburgh, Pittsburgh, PA 15213, USA

[2]The Genomics and Proteomics Core Laboratories, University of Pittsburgh, Pittsburgh, PA 15213, USA

[3]The McGowan Institute for Regenerative Medicine, University of Pittsburgh, Pittsburgh, PA 15213, USA

[4]The Center for Neuroscience, University of Pittsburgh, Pittsburgh, PA 15213, USA

Abstract

Mitochondrial transcription factor A (TFAM) regulates mitochondrial biogenesis, which is downregulated by extracellular signal-regulated protein kinases (ERK1/2) in cells treated chronically with the complex I inhibitor 1-methyl-4-phenylpyridinium (MPP+). We utilized mass spectrometry to identify ERK1/2-dependent TFAM phosphorylation sites. Mutation of TFAM at serine 177 to mimic phosphorylation recapitulated the effects of MPP+ in decreasing the binding of TFAM to the light strand promoter, suppressing mitochondrial transcription. Mutant TFAM was unable to affect respiratory function or rescue the effects of MPP+ on respiratory complexes. These data disclose a novel mechanism by which ERK1/2 regulates mitochondrial function through direct phosphorylation of TFAM.

Keywords

MAP kinases; phosphorylation; mitochondrial biogenesis; Parkinson disease

1. Introduction

Changes in cellular differentiation and metabolic state are accompanied by altered mitochondrial function in both health and disease. In particular, downregulation of mitochondrial respiration are hallmarks of neoplastic transformation and neurodegenerative diseases (Hsu and Sabatini, 2008; Johri and Beal, 2012). Although decreased nuclear

*Correspondence to Charleen T. Chu: ctc4@pitt.edu. Tel: 412-383-5379.
†Current addresses:
RKD, Department of Pharmacology, University of Nevada, Reno, Reno, NV, 89557; SJC: Division of Biological Sciences, University of California, San Diego; AMG: Department of Neurology and Neuroscience, Weill Cornell Medical College, New York, NY 10065

PGC-1α related gene transcription has been implicated in Parkinson's disease (Zheng et al., 2010) along with increased mitophagy (Zhu et al., 2007), regulatory mechanisms that signal increased mitochondrial clearance or decreased mitochondrial biogenesis remain incompletely described.

The mitochondrial transcription factor A (TFAM) is one of the central regulatory components of mitochondrial nucleoids (Spelbrink, 2010). TFAM contains two high mobility group (HMG) domains, and is targeted to the mitochondrion via an N-terminal canonical mitochondrial target sequence (MTS). Following mitochondrial import, the MTS of the TFAM precursor is cleaved to form mature TFAM (Parisi and Clayton, 1991). In the matrix, TFAM interacts with mitochondrial DNA (mtDNA) to stabilize the mitochondrial genome (Alam et al., 2003; Murphy and Churchill, 2000) and binds the D-loop to regulate the bidirectional transcription of mtDNA from light and heavy strand promoters (LSP, HSP1 and HSP2) (Fisher and Clayton, 1988; Fisher et al., 1987). Not only does TFAM recruit TFB2M and mitochondrial RNA polymerase for transcriptional activation (Dairaghi et al., 1995; McCulloch and Shadel, 2003), but also bends the LSP DNA to open the transcription start site (Ngo et al., 2011; Rubio-Cosials et al., 2011).

With the exception of a beneficial effect on obesity and insulin resistance (Vernochet et al., 2012), most tissues in conditional TFAM knockout mice exhibit detrimental phenotypes accompanied by impaired mitochondrial function (Ekstrand et al., 2007; Li et al., 2000; Silva et al., 2000). However, the molecular mechanisms by which TFAM function is regulated under physiological or pathological conditions have yet to be fully elucidated. Chronic challenge of neuronal cells with lower doses of the complex I inhibitor 1-methyl-4-phenylpyridinium (MPP+) results in suppression of mitochondrial biogenesis and induction of mitophagy (Zhu et al., 2012). Inhibiting ERK activation restores mitochondrial content and function to a much greater extent than manipulating mitophagy, suggesting an important effect on mitochondrial biogenesis. In this study, we discovered that TFAM is a direct target of ERK phosphorylation. Mimicking the ERK-mediated phosphorylation of serine 177 (S177) impairs the ability of TFAM to associate with the LSP, with consequent effects on the regulation of mitochondrial transcript levels, mitochondrial respiration and respiratory subunit expression.

2. Materials and Methods

2.1. Cell lines and treatments

SH-SY5Y cells (ATCC, Manassas, VA) were cultured in Advanced Dulbecco's modified Eagle's medium supplemented with 5% heat-inactivated fetal calf serum (BioWhittaker, Walkersville, MD), 2mM L-glutamine and 10mM HEPES. Prior to chronic treatment, SH-SY5Y cells were differentiated with 10μM retinoic acid (RA) (Sigma Aldrich, St Louis, MO) for 72 h and the same concentration of RA was maintained during the entire procedure (Simpson et al., 2001). HEK293 cells (ATCC, Manassas, VA) were maintained at 37°C, 5% CO2 in Dulbecco's modified Eagle's medium (BioWhittaker, Walkersville, MD) supplemented with 5% heat-inactivated fetal calf serum (Invitrogen, Carlsbad, CA), 2mM glutamine and 10mM HEPES. Reagents used for chronic treatment were 0.1% DMSO (Fisher Scientific, Pittsburgh, PA), 250 μM MPP+ (Sigma Aldrich, St Louis, MO), 10μM

1,4-diamino-2,3-dicyano-1,4-bis[2-aminophenylthio] butadiene (U0126) (Promega, Madison, WI, USA), or a combination of 250 μM MPP+ and 10μM U0126 which were reapplied every 48 h for the indicated time points.

2.2. Plasmids and siRNAs

The human HA tagged TFAM (TFAM-HA) expression plasmid was subcloned by replacing the turbo GFP coding sequence with a HA-tag in the TFAM-tGFP plasmid (Origene Technologies, Inc., Rockville, MD). TFAM(S177D)-HA and TFAM(S177A)-HA were engineered using the Quickchange II XL site-directed mutagenesis kit (Agilent Technology, Inc., La Jolla, CA) according to the manufacturer's instructions. GST-TFAM was subcloned by inserting the cDNA of TFAM into the StyI and XhoI restriction sites of pGEX 6p-1 (GE Healthcare Bio-Sciences Corp., Piscataway, NJ). Other expression plasmids used in this study include: constitutively activated ERK2 (ERK2CA-pCMV5), and dominant negative (kinase deficient) ERK2 (ERK2DN-pCMV5) have been previously described (Dagda et al., 2008; Emrick et al., 2001). The siRNAs used for endogenous TFAM knockdown were a 1:1 mix pool of two pre-validated siRNAs which specifically recognize the 3' end untranslated region (3'-UTR) of human TFAM mRNA. The forward sequences of these siRNA are: 5'-GACUUCUGCCAGCAUAAUAdTdT-3' and 5'- GAACUCAUCUAGGUAAAU UdTdT-3' (Sigma Aldrich, St Louis, MO).

2.3. Transfection

Lipofectamine 2000 (Life Technologies, Grand Island, NY) was used at a ratio of 3 μl per μg for plasmid and at a ratio of 1 μl per 20 pmol for siRNA transfection. The media was changed 6 h after transfection.

2.4. Immunoprecipitation, Western Blot and two-dimensional (2D) electrophoresis analysis

After indicated treatments, cells were harvested and lysed in a lysis buffer containing 1% triton X-100 containing protease and phosphatase inhibitors. HA-tagged TFAM or mutant proteins were immunoprecipitated by incubating cell lysates with an anti-HA antibody (Miltenyi Biotec. Inc., Auburn, CA) and purified according to the manufacturer's instructions. Protein concentration was determined by Coomassie Blue Protein Assay (Pierce, Rockford, IL). Western blot analysis was performed as described previously (Zhu et al., 2012). The post-translational modification of TFAM was analyzed by 2D immunoblotting procedures using an isoelectric focusing (IEF) apparatus and IPG strips pH 3–10 (Protean IEF Cell, Bio-Rad) followed by SDS-PAGE and immunoblotting, according to the manufacturer's instructions. For immunoblotting, rabbit anti-TFAM antibody (1:1,000, Cell Signaling Tech., Beverly, MA, USA; 1:10,000, Dr. C. Cameron, Penn State University), mouse anti-phospho-ERK1/2 (1:1000, Cell Signaling Tech., Beverly, MA, USA), rabbit anti-ERK1/2 (1:10, 000, Millipore, Billerica, MA, USA), mouse anti-human mitochondrial antigen of 60KD (1:1,000, Biogenex, San Ramon, CA), rabbit anti-human TOM20 (1:10, 000, Santa Cruz Biotechnology, Santa Cruz, CA, USA), mouse anti-HA (1:1,000, Covance, Denver, PA), rabbit anti-GAPDH (1:10,000, Abcam, Cambridge, MA), mouse anti-α-tubulin (1:10,000, Abcam, Cambridge, MA), rabbit anti-laminin A/C (1:1,000, Cell Signaling Tech, Beverly, MA, USA). Densitometry of specific immunoreactive bands was quantified by using Image J version 1.44 (NIH, Bethesda, MD).

2.5. Alkaline phospatase (AP) treatment of proteins from cell lysate

After indicated treatments, cells were lysed in a buffer containing 1% triton X-100 and protease inhibitors. Phosphoproteins in the supernatant were dephosphorylated with 10 units of AP (Roche Applied Science, Indianapolis, IN) per 100 μg of total protein at 37°C for 1 h.

2.6. Preparation of GST-TFAM protein

A glycerol stock of *E. coli* transformed with TFAM-pGEX 6P-1 was grown in LB-Broth at 37°C, 250 rpm to 0.6 at OD_{600}. To induce expression of the recombinant protein, IPTG (Thermo Scientific, Pittsburgh, PA) was added into the LB media at a final concentration of 0.1 mM for 3 h. The bacterial pellet was harvested and resuspended in PBS. The GST-TFAM recombinant protein was released in *E. coli* cells by sonication and purified in a glutathione-agarose column (Thermo Scientific, Pittsburgh, PA) according to the manufacturer's procedures.

2.7. In vitro phosphorylation assay of TFAM

For the *in vitro* phosphorylation reaction, 1–2 μg GST-TFAM, 100 units of activated recombinant ERK2 (New England BioLabs Inc., Ipswich, MA), 200μM ATP and 300 μCi/μmol γ-^{32}P-ATP (PerkinElmer, Waltham, MA) were incubated in 1× Protein Kinase NEBuffer (New England BioLabs Inc., Ipswich, MA) in a total volume of 30 μl and at 30°C for 1 h. Reactions were terminated by adding 10 μl 4× SDS-PAGE sample buffer and heating the samples at 75°C for 20 min. Following 4–15% SDS-PAGE, protein bands were visualized with Coomassie Blue R-250 staining, gels were dried and ^{32}P incorporation measured by autoradiography.

2.8. Mass spectrometric (MS) sample preparation and analysis

GST-TFAM protein from *in vitro* kinase reactions employing nonradioactive ATP or *in vivo* phosphorylated TFAM-HA protein immunoprecipitated from SH-SY5Y cells were resolved by SDS-PAGE. Gel bands were excised, destained, reduced with Tris(2-carboxyethyl)phosphine hydrochloride (TCEP) (Sigma Aldrich, St Louis, MO), alkylated with iodoacetamide (Sigma Aldrich, St Louis, MO), digested with trypsin or chymotrypsin, and extracted as previously described (Shevchenko et al., 2006). Protein identification of TFAM was confirmed using a 4800 MALDI TOF/TOF Analyzer (ABSciex, Framingham, MA) and database searching using ProteinPilot and the Mascot search engine. Phosphorylation sites were identified by LC-MS/MS (nanoAcquity UPLC, Waters; LTQ Orbitrap Velos, Thermo Fisher Scientific, San Jose, CA) followed by data analysis with Proteome Discoverer using SEQUEST for peptide identification and the PhosphoRS algorithm for phosphosite probabilities.

2.9. TFAM-LSP DNA and mtDNA binding assay

After the indicated treatments, cells ($3–5\times10^6$) were harvested and lysed in 150 mM NaCl, 1% Triton X-100, 50 mM TrisHCl, supplemented with protease and phosphatase inhibitors, pH 8.0. The supernatant was recovered and incubated with either a biotinylated LSP DNA probe (hereafter: biotin-LSP) that consists of a double stranded DNA oligo containing a TFAM consensus sequence derived from the LSP (Forward sequence: 5'-biotin-

tgtgttagttgggggtgactgttaaa-3', Reverse sequence: 5'-tttaacagtcacccccaactaacaca-3') or a non-specific biotinylated mtDNA probe derived from a coding region of ND1 (Forward sequence: 5'-biotin-actacaacccttcgctgacgc cataaaactcttca-3', Reverse sequence: 5'-tgaagagttttatggcgtcagcgaagggttgtagt-3'). Following incubation at 4°C for 1 h, 60 μL of streptavidin conjugated magnet beads (Sigma Aldrich), were added and incubated for 1 h. The TFAM-DNA complex pulled down by the streptavidin-beads was isolated by centrifugation at 6,000 rpm for 1 min, washed with lysis buffer (3 × 300 μL), and eluted with 1× SDS-PAGE sample buffer. Proteins from pull-down and lysate (input) were resolved by 12% SDS-PAGE followed by Western Blot analysis. The relative protein abundance was analyzed by Image J densitometry. Relative binding of TFAM was calculated as the ratio of the amount of TFAM protein identified in the pull-down fraction normalized to input levels.

2.11. In vivo mitochondrial DNA content and transcript level assay

To test the impact of TFAM and its phosphorylation site mutants on mtDNA content and mitochondrial transcript levels, HEK293 cells were first transfected with siRNA to knockdown endogenous TFAM, followed by transfection at 24 h with TFAM-HA wild type or mutant plasmid for another 48 h. Genomic DNA was prepared by using a genomic DNA purification kit (Promega, Madison, WI). mtDNA content was analyzed by Sybr green quantitative PCR (qPCR) using primers amplifying ND1(Forward, 5'-cacccaagaacagggtttgt-3', Reverse, 5'-tggccatgggatagttgttaa-3') normalized to ACTB (forward, 5'-ggcatcctcaccctgaagta-3', reverse, 5'-gaaggtgtggtgccagattt-3'). Total RNA was extracted by using an RNeasy kit (Qiagen, Valencia, CA) according to the manufacturer's instructions. cDNA was produced by reverse transcription reaction with the GeneAmp RNA PCR kit (Life Technologies, Grand Island, NY) and further quantified by qPCR using individual TaqMan probes (Life Technologies, Grand Island, NY). The levels of mitochondrial transcripts were analyzed by quantitative RT-PCR using individual TaqMan probes (ND6 (Hs02596879_g1), RNR2 (Hs02596860-s1) and ND1 (Hs0259873-s1) normalized to GAPDH mRNA (4333764F). Among these transcripts, ND6 mRNA was transcribed by LSP1, RNR2 by HSP1, and ND1 by HSP2.

2.12. Mitochondrial respiratory chain activity assay

HEK293 cells were transfected with either control vector or the indicated TFAM-HA plasmids for 24 h, and then transferred to XF24 V7 Cell Culture Microplates at a density of 100,000 cells/well for 24 hours prior to oxygen consumption rate (OCR) analysis. Mitochondrial OCRs were analyzed using a XF24 Extracellular Flux Analyzer (Seahorse Bioscience, North Billerica, MA) at baseline and following the sequential addition of 1 μM oligomycin, 300 nM FCCP, and 1 μM antimycin A to determine OCR-coupled to ATP synthesis, respiratory reserve capacity and non-mitochondrial OCR, respectively. Data were analyzed and graphed using the R project for statistical computing.

3. Results

3.1. Identification of ERK-directed phosphorylation of TFAM in cells and in vitro

To test the hypothesis that TFAM function can be regulated by post-translational modification, we analyzed TFAM by 2D-immunoblotting. Chronic MPP+ treatment elicited the appearance of TFAM immunoreactive spots exhibiting more acidic isoelectric points (pI). This effect was reversed by U0126, which inhibits the activation of ERK, or by expression of a dominant negative ERK2 mutant (ERK2-DN). Moreover, incubation of MPP + treated cell lysates with alkaline phosphatase (AP) resulted in disappearance of these acidic forms of TFAM (Fig. 1A). Collectively, these data implicate ERK-dependent phosphorylation of TFAM.

To identify specific residues of TFAM that undergo ERK-dependent phosphorylation in living cells, we co-transfected a TFAM-HA plasmid with either a constitutively active ERK2 (ERK2-CA) plasmid or its vector control. TFAM-HA proteins were immunoprecipitated with anti-HA conjugated magnetic beads and resolved by SDS-PAGE. The Coomassie-stained gel bands of 31kD and 26 kD were excised for in-gel digestion with trypsin and analyzed by MALDI-TOF/TOF mass spectrometry. The 31kD band was confirmed as the precursor form and the 26 kD band as the mature form of TFAM (Fig. 2A–C). To identify phosphorylated residues on TFAM, we analyzed the tryptic peptides from the TFAM-HA precursor band by LC-MS/MS. A phosphopeptide was identified in which serine (S177) in the 2nd HMG domain was phosphorylated in cells transiently expressing ERK2-CA (Fig. 3A & B). The same modification was not detected in control cells only expressing TFAM-HA. Examination of the sequence reveals proline in the P+1 position, as favored by proline-directed kinases such as ERK1/2.

Next, we performed *in vitro* kinase reactions to investigate whether TFAM is a direct ERK substrate. Following incubation with recombinant ERK2, a 50 KD and a 38 KD band gained P^{32}(Fig. 1B). Employing MALDI-TOF/TOF-MS, the 50 KD band was identified as the full-length form of GST-TFAM, while the 38 KD band appeared to be a C-terminally truncated form of GST-TFAM, as no peptides after residue 133 were detected (Fig. 4A & B). To identify the serine/threonine residues of TFAM directly phosphorylated by ERK2, we analyzed the digested peptides by LC-MS/MS. The same proline-directed phosphorylation site S177 identified from cells expressing ERK2-CA (Fig. 3), was also detected in the *in vitro* kinase reaction product (Fig. 4C). Specificity of the kinase reactions for the TFAM portion of the fusion protein was supported by the fact that none of the phospho-peptides identified by LC/MS-MS were derived from the GST-tag.

3.2. ERK-dependent phosphorylation of TFAM at HMG2 impairs its LSP binding

TFAM specifically binds the LSP within the D-loop region of mtDNA, and such interaction is necessary to activate bidirectional mtDNA transcription by both promoters (Fisher et al., 1987; Shi et al., 2012). Based on crystal structure data (Ngo et al., 2011; Rubio-Cosials et al., 2011), we examined a rendered image of the TFAM-LSP DNA interaction complex, noting that TFAM residues 177–179 are bound to the minor groove of the DNA (Fig. 5A). Therefore, we reasoned that phosphorylation of S177 may interfere with TFAM-DNA

binding. We applied a DNA-protein pull-down assay to the chronic MPP+ cell model in the presence or absence of a MEK inhibitor U0126. After indicated treatments, SH-SY5Y cells were lysed and incubated with a biotinylated DNA probe derived from the LSP TFAM consensus sequence inside the D-loop region (Shi et al., 2012). As shown in Fig. 5B, the binding of endogenous TFAM to the LSP DNA probe was reduced by MPP+ treatment by 35% relative to control, and this was completely reversed by co-treatment with U0126. We further investigated the involvement of ERK by transfecting with either constitutively active ERK2CA-GFP or inactive ERK2DN-GFP. Expression of ERK2CA-GFP caused TFAM to exhibit reduced binding to LSP DNA (Fig. 5C).

To analyze whether the ERK-directed phosphorylation of serine 177 could contribute to reduced DNA binding of TFAM, we transiently transfected plasmids coding for wild-type and the phosphomimetic S177D mutant. In contrast to wild-type TFAM, the binding of TFAM-177D to LSP was significantly reduced (Fig. 5D). To validate the binding specificity between TFAM and the LSP DNA in this assay, we used either non-labeled LSP DNA to compete the biotinylated LSP probe for binding with TFAM or free biotin to block the interaction of the biotin-LSP- TFAM complex with streptavidin beads. Both effectively abolished the pull-down of TFAM (Fig.6A). The phosphorylation resistant TFAM-S177A mutant also displayed reduced binding to LSP, suggesting that the hydroxyl group of serine 177 is important for TFAM-LSP DNA complex formation. In addition to selective binding of TFAM to mtDNA promoters, TFAM is capable of interacting nonselectively with mtDNA (Alam et al., 2003; Murphy and Churchill, 2000). Interestingly, there was no significant difference observed between wild-type TFAM, TFAM-S177D and TFAM-S177A for binding to a general mtDNA probe derived from the coding region of ND1, which argues that phosphorylation of serine 177 does not affect the capacity of TFAM to package mtDNA (Fig.6B).

3.3. TFAM(177D) fails to restore mtDNA transcript levels in cells with reduced endogenous TFAM

To assess the impact of ERK-mediated phosphorylation of TFAM on mtDNA transcription, we transfected cells with a mixture of two validated siRNAs targeting the 3’ UTR of TFAM mRNA to reduce the expression of endogenous TFAM, followed by co-expression of the indicated RNAi-resistant wild-type and phosphomimetic TFAM mutants (Fig. 7A). Since TFAM is centrally important for packaging and stabilizing mtDNA, we first analyzed the content of mtDNA. In agreement with the results shown in Fig.6B, overexpression of TFAM, S177D or S177A each effectively restored the loss of mtDNA content incurred by knockdown of endogenous TFAM to similar levels (Fig.7B). On the other hand, the relative levels of mitochondrial RNA transcription driven by the LSP, HSP1 and HSP2 were estimated by quantifying their transcripts, ND6, RNR2 and ND1, respectively, using quantitative RT-PCR. The levels of all three mRNAs were significantly reduced when endogenous TFAM was knocked down, but rescued by restoring wild-type TFAM-HA, indicating that TFAM is necessary for driving transcription at the LSP, HSP1 and HSP2. In contrast, S177D and S177A, which are impaired in LSP binding (Fig. 6A), failed to rescue the suppression of mtDNA transcripts induced by the loss of endogenous TFAM protein (Fig.7B–D).

3.4. TFAM phosphorylation leads to impaired ability to regulate mitochondrial function

We examined the effects of TFAM phosphomimetic mutants on mitochondrial respiration. While expression of the wild-type protein robustly enhanced the basal oxygen consumption rate (OCR) and the maximal respiratory capacity after FCCP treatment, the S177D mutant failed to show this effect (Fig. 8A). We previously reported that MPP+ treatment induces mitophagy accompanied by decreased expression of mitochondrial respiratory complex proteins (Zhu et al., 2012; Zhu et al., 2007). Overexpression of wild-type TFAM can completely rescue the loss of respiratory complex proteins, in the chronic MPP+ model, restoring mitochondrial protein synthesis. (Zhu et al., 2012). In the current study, cells transfected with TFAM-HA or the phosphomimetic TFAM (S177D) mutant were treated with a higher dose of MPP+ for 24 h. Mitochondrial content was analyzed by immunoblotting for proteins from each of the five respiratory chain complexes. While overexpression of TFAM-HA partially reversed the loss of respiratory chain proteins caused by this acute injury, transient expression of TFAM(S177D)-HA was incapable of doing so (Fig. 8B–E). These data suggest that ERK-mediated phosphorylation of TFAM at S177 suppresses its ability to participate in compensatory mitochondrial biogenesis during injury.

4. Discussion

Increasing evidence indicates that ERK signaling regulates mitochondrial function and content (Monick et al., 2008; Nowak et al., 2006). In cancer cells, ERK reduces mitochondrial respiration while promoting glycolytic metabolism to provide metabolic intermediates compatible with rapid growth (Marko et al., 2010; Nowak et al., 2006). ERK2 upregulates mitophagy in several models of parkinsonian neurodegeneration (Dagda et al., 2008), while suppressing translation of mtDNA coded proteins in the chronic MPP+ model (Zhu et al., 2012). In the current study, we identified TFAM as a direct substrate of ERK signaling. Specifically, phosphorylation at S177 contributes to suppression of mitochondrial biogenesis, revealing a second mechanism other than mitophagy by which ERK downregulates mitochondria.

The mitochondrial genome contains three promoters. Transcription initiated from the LSP produces ND6 and some tRNAs; the HSP1 regulates two rRNAs and the remaining twelve tRNAs, while twelve proteins are transcribed using HSP2 (Bonawitz et al., 2006; Shadel, 2008). As previously reported (Fisher et al., 1987; Shi et al., 2012), TFAM positively regulated transcription initiated from all three promoters. However, the phosphomimetic mutant TFAM(177D) showed reduced affinity for promoter binding, losing the ability to rescue phenotypes caused by loss of endogenous TFAM (Fig. 5–7). Such ERK-mediated loss of TFAM function would be predicted to result in dysfunctional mitochondria, as supported by studies showing that expression of ERK2-CA drives mitochondrial degradation (Dagda et al., 2008).

A recent study showed that TFAM was phosphorylated by protein kinase A (PKA) in the HMG1 domain (S55, S56 and S61) in cells co-expressing TFAM and PKA, resulting in inability to bind LSP and Lon-mediated degradation (Lu et al., 2013). In contrast, mutating the ERK-dependent phosphorylation site in the HMG2 domain showed no consistent effects on TFAM expression levels, and the LSP binding of TFAM(S177D) or TFAM(S177A) was

impaired, but not abolished. Our data argues that the hydroxyl group of serine 177 is involved in a specific interaction between TFAM and LSP, as there is no effect of S177 mutation on nonselective interactions with non-promoter mtDNA. It is possible that S177 is important for DNA bending, as bending of the LSP DNA is required for TFAM regulated transcriptional activation. Overall, these observations suggest that reduced transcriptional activity plays a more important role than decreased protein stability in the biological effects attributed to phosphorylation at serine 177.

We have previously shown that ERK may translocate to the mitochondria after cytosolic activation (Dagda et al., 2008), or it can be activated *in situ* by mitochondrial ROS (Kulich et al., 2007). Phosphorylation of serine 177 could occur in either location as it was identified on both precursor and mature TFAM isolated from cells experiencing increased ERK activity.

The RAS/RAF/MEK/ERK pathway is one of the major pathways involved in tumorigenesis associated with the Warburg effect (Hall et al., 2013). Interestingly, ERK kinase activity is also elevated within human post-mortem midbrain tissues from Parkinson's disease and Lewy body dementia patients, and phosphorylated ERK is observed specifically within degenerating neurons (Zhu et al., 2003; Zhu et al., 2002). In addition, mutations in the leucine rich repeat kinase 2, a relatively common cause of autosomal dominant Parkinson's disease, drives ERK1/2 activation (Carballo-Carbajal et al., 2010; Plowey et al., 2008; Reinhardt et al., 2013). Thus, the suppressive effects of ERK-mediated TFAM phosphorylation on mtDNA transcription may contribute to reduced mitochondrial levels or regenerative capacity observed in Parkinson's disease.

In conclusion, this study indicates that TFAM is a direct substrate of ERK, with the S177 site regulating its DNA promoter binding and transcriptional function. This not only lends further insight into post-translational mechanisms by which cellular signaling pathways can modulate mitochondrial biogenesis, but also may contribute to decreased mitochondrial function observed in neoplastic and neurodegenerative diseases characterized by ERK activation.

Acknowledgments

We thank Ms. Danielle Hu for assistance in preparing some of the TFAM-HA plasmids and Dr. Ben Van Houten, University of Pittsburgh, for consultation and use of the Seahorse XF24 Flux Analyzer.

This work was supported by the National Institutes of Health (R01 AG026389, R01 NS065789 and K18 DC009120). The Genomics and Proteomics Core Laboratories and Biomedical Mass Spectrometry Center were supported in part by UL1 RR024153, UL1 TR000005 and P30 CA047904. The funding agencies were not involved in the study design, collection and interpretation of the data, writing of the report, or the decision to submit for publication.

REFERENCES

Bonawitz ND, Clayton DA, Shadel GS. Initiation and beyond: multiple functions of the human mitochondrial transcription machinery. Mol Cell. 2006; 24:813–825. [PubMed: 17189185]

Carballo-Carbajal I, Weber-Endress S, Rovelli G, Chan D, Wolozin B, Klein CL, Patenge N, Gasser T, Kahle PJ. Leucine-rich repeat kinase 2 induces alpha-synuclein expression via the extracellular signal-regulated kinase pathway. Cell Signal. 2010; 22:821–827. [PubMed: 20074637]

Dagda RK, Zhu J, Kulich SM, Chu CT. Mitochondrially localized ERK2 regulates mitophagy and autophagic cell stress: implications for Parkinson's disease. Autophagy. 2008; 4:770–782. [PubMed: 18594198]

Dairaghi DJ, Shadel GS, Clayton DA. Addition of a 29 residue carboxyl-terminal tail converts a simple HMG box-containing protein into a transcriptional activator. J Mol Biol. 1995; 249:11–28. [PubMed: 7776365]

Ekstrand MI, Terzioglu M, Galter D, Zhu S, Hofstetter C, Lindqvist E, Thams S, Bergstrand A, Hansson FS, Trifunovic A, et al. Progressive parkinsonism in mice with respiratory-chain-deficient dopamine neurons. Proc Natl Acad Sci U S A. 2007; 104:1325–1330. [PubMed: 17227870]

Emrick MA, Hoofnagle AN, Miller AS, Ten Eyck LF, Ahn NG. Constitutive activation of extracellular signal-regulated kinase 2 by synergistic point mutations. J Biol Chem. 2001; 276:46469–46479. [PubMed: 11591711]

Fisher RP, Clayton DA. Purification and characterization of human mitochondrial transcription factor 1. Mol Cell Biol. 1988; 8:3496–3509. [PubMed: 3211148]

Fisher RP, Topper JN, Clayton DA. Promoter selection in human mitochondria involves binding of a transcription factor to orientation-independent upstream regulatory elements. Cell. 1987; 50:247–258. [PubMed: 3594571]

Hall A, Meyle KD, Lange MK, Klima M, Sanderhoff M, Dahl C, Abildgaard C, Thorup K, Moghimi SM, Jensen PB, et al. Dysfunctional oxidative phosphorylation makes malignant melanoma cells addicted to glycolysis driven by the (V600E)BRAF oncogene. Oncotarget. 2013; 4:584–599. [PubMed: 23603840]

Hsu PP, Sabatini DM. Cancer cell metabolism: Warburg and beyond. Cell. 2008; 134:703–707. [PubMed: 18775299]

Johri A, Beal MF. Mitochondrial dysfunction in neurodegenerative diseases. J Pharmacol Exp Ther. 2012; 342:619–630. [PubMed: 22700435]

Kulich SM, Horbinski C, Patel M, Chu CT. 6-Hydroxydopamine induces mitochondrial ERK activation. Free Radic Biol Med. 2007; 43:372–383. [PubMed: 17602953]

Li H, Wang J, Wilhelmsson H, Hansson A, Thoren P, Duffy J, Rustin P, Larsson NG. Genetic modification of survival in tissue-specific knockout mice with mitochondrial cardiomyopathy. Proc Natl Acad Sci U S A. 2000; 97:3467–3472. [PubMed: 10737799]

Lu B, Lee J, Nie X, Li M, Morozov YI, Venkatesh S, Bogenhagen DF, Temiakov D, Suzuki CK. Phosphorylation of human TFAM in mitochondria impairs DNA binding and promotes degradation by the AAA+ Lon protease. Mol Cell. 2013; 49:121–132. [PubMed: 23201127]

Marko AJ, Miller RA, Kelman A, Frauwirth KA. Induction of glucose metabolism in stimulated T lymphocytes is regulated by mitogen-activated protein kinase signaling. PLoS One. 2010; 5:e15425. [PubMed: 21085672]

McCulloch V, Shadel GS. Human mitochondrial transcription factor B1 interacts with the C-terminal activation region of h-mtTFA and stimulates transcription independently of its RNA methyltransferase activity. Mol Cell Biol. 2003; 23:5816–5824. [PubMed: 12897151]

Monick MM, Powers LS, Barrett CW, Hinde S, Ashare A, Groskreutz DJ, Nyunoya T, Coleman M, Spitz DR, Hunninghake GW. Constitutive ERK MAPK activity regulates macrophage ATP production and mitochondrial integrity. J Immunol. 2008; 180:7485–7496. [PubMed: 18490749]

Ngo HB, Kaiser JT, Chan DC. The mitochondrial transcription and packaging factor Tfam imposes a U-turn on mitochondrial DNA. Nat Struct Mol Biol. 2011; 18:1290–1296. [PubMed: 22037171]

Nowak G, Clifton GL, Godwin ML, Bakajsova D. Activation of ERK1/2 pathway mediates oxidant-induced decreases in mitochondrial function in renal cells. Am J Physiol Renal Physiol. 2006; 291:F840–F855. [PubMed: 16705147]

Parisi MA, Clayton DA. Similarity of human mitochondrial transcription factor 1 to high mobility group proteins. Science. 1991; 252:965–969. [PubMed: 2035027]

Plowey ED, Cherra SJ 3rd, Liu YJ, Chu CT. Role of autophagy in G2019S-LRRK2-associated neurite shortening in differentiated SH-SY5Y cells. J Neurochem. 2008; 105:1048–1056. [PubMed: 18182054]

Reinhardt P, Schmid B, Burbulla LF, Schondorf DC, Wagner L, Glatza M, Hoing S, Hargus G, Heck SA, Dhingra A, et al. Genetic correction of a LRRK2 mutation in human iPSCs links parkinsonian

neurodegeneration to ERK-dependent changes in gene expression. Cell Stem Cell. 2013; 12:354–367. [PubMed: 23472874]

Rubio-Cosials A, Sidow JF, Jimenez-Menendez N, Fernandez-Millan P, Montoya J, Jacobs HT, Coll M, Bernado P, Sola M. Human mitochondrial transcription factor A induces a U-turn structure in the light strand promoter. Nat Struct Mol Biol. 2011; 18:1281–1289. [PubMed: 22037172]

Shadel GS. Expression and maintenance of mitochondrial DNA: new insights into human disease pathology. Am J Pathol. 2008; 172:1445–1456. [PubMed: 18458094]

Shevchenko A, Tomas H, Havlis J, Olsen JV, Mann M. In-gel digestion for mass spectrometric characterization of proteins and proteomes. Nat Protoc. 2006; 1:2856–2860. [PubMed: 17406544]

Shi Y, Dierckx A, Wanrooij PH, Wanrooij S, Larsson NG, Wilhelmsson LM, Falkenberg M, Gustafsson CM. Mammalian transcription factor A is a core component of the mitochondrial transcription machinery. Proc Natl Acad Sci U S A. 2012; 109:16510–16515. [PubMed: 23012404]

Silva JP, Kohler M, Graff C, Oldfors A, Magnuson MA, Berggren PO, Larsson NG. Impaired insulin secretion and beta-cell loss in tissue-specific knockout mice with mitochondrial diabetes. Nat Genet. 2000; 26:336–340. [PubMed: 11062475]

Simpson PB, Bacha JI, Palfreyman EL, Woollacott AJ, McKernan RM, Kerby J. Retinoic acid evoked-differentiation of neuroblastoma cells predominates over growth factor stimulation: an automated image capture and quantitation approach to neuritogenesis. Anal Biochem. 2001; 298:163–169. [PubMed: 11757502]

Spelbrink JN. Functional organization of mammalian mitochondrial DNA in nucleoids: history, recent developments, and future challenges. IUBMB Life. 2010; 62:19–32. [PubMed: 20014006]

Vernochet C, Mourier A, Bezy O, Macotela Y, Boucher J, Rardin MJ, An D, Lee KY, Ilkayeva OR, Zingaretti CM, Emanuelli B, Smyth G, Cinti S, Newgard CB, Gibson BW, Larsson NG, Kahn CR. Adipose-specific deletion of TFAM increases mitochondrial oxidation and protects mice against obesity and insulin resistance. Cell Metab. 2012; 16:765–676. [PubMed: 23168219]

Zheng B, Liao Z, Locascio JJ, Lesniak KA, Roderick SS, Watt ML, Eklund AC, Zhang-James Y, Kim PD, Hauser MA, et al. PGC-1alpha, a potential therapeutic target for early intervention in Parkinson's disease. Sci Transl Med. 2010; 2:52ra73.

Zhu JH, Guo F, Shelburne J, Watkins S, Chu CT. Localization of phosphorylated ERK/MAP kinases to mitochondria and autophagosomes in Lewy body diseases. Brain Pathol. 2003; 13:473–481. [PubMed: 14655753]

Zhu JH, Gusdon AM, Cimen H, Van Houten B, Koc E, Chu CT. Impaired mitochondrial biogenesis contributes to depletion of functional mitochondria in chronic MPP+ toxicity: dual roles for ERK1/2. Cell Death Dis. 2012; 3:e312. [PubMed: 22622131]

Zhu JH, Horbinski C, Guo F, Watkins S, Uchiyama Y, Chu CT. Regulation of autophagy by extracellular signal-regulated protein kinases during 1-methyl-4-phenylpyridinium-induced cell death. Am J Pathol. 2007; 170:75–86. [PubMed: 17200184]

Zhu JH, Kulich SM, Oury TD, Chu CT. Cytoplasmic aggregates of phosphorylated extracellular signal-regulated protein kinases in Lewy body diseases. Am J Pathol. 2002; 161:2087–2098. [PubMed: 12466125]

Highlights

- TFAM is phosphorylated by ERK1/2 at S177 in cells treated chronically with MPP+.
- Phosphorylation reduces TFAM binding to the mitochondrial light strand promoter.
- The phosphomimetic TFAM S177D mutant is unable to rescue mtDNA transcript levels.
- This represents a novel mechanism by which ERK1/2 regulates mitochondrial activity.

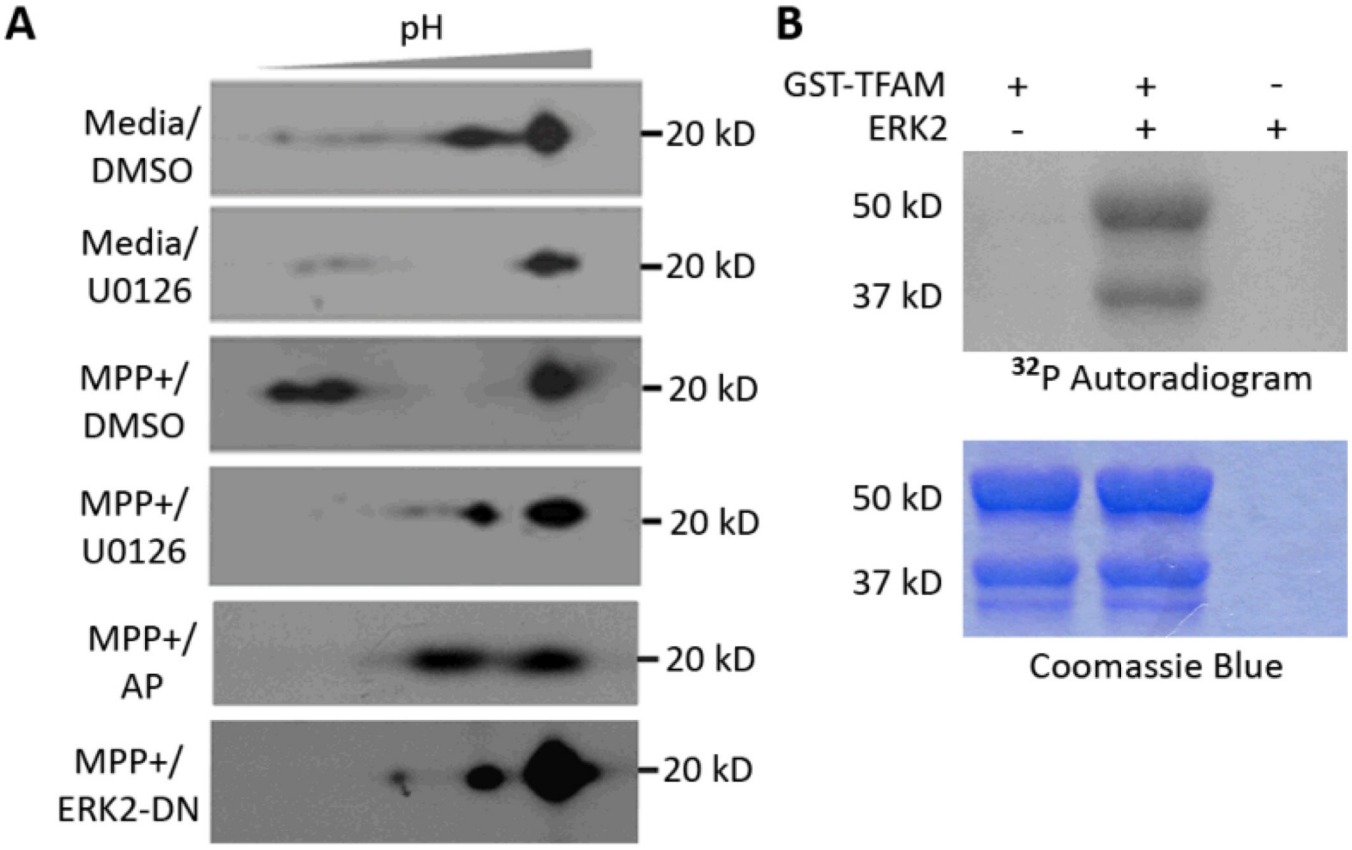

Fig. 1.

ERK-dependent phosphorylation of TFAM. (A) Retinoic acid-differentiated SH-SY5Y cells were treated with the indicated reagents for 6 days prior to analysis. TFAM post-translational modification was analyzed by 2-D immunoblotting using an anti-TFAM antibody. Media is the negative control for MPP+ and DMSO is the negative control for U0126. MPP+/AP indicates MPP+ treated cell lysates that were incubated *in vitro* with alkaline phosphatase (AP); MPP+/ ERK2-DN refers to MPP+ treatment of cells expressing a dominant negative ERK2. (B) *In vitro* phosphorylation was performed using recombinant active ERK2 and GST-TFAM as the substrate in the presence of ^{32}P-labeled ATP and detected using autoradiography. Protein loading was visualized by Coomassie Blue staining.

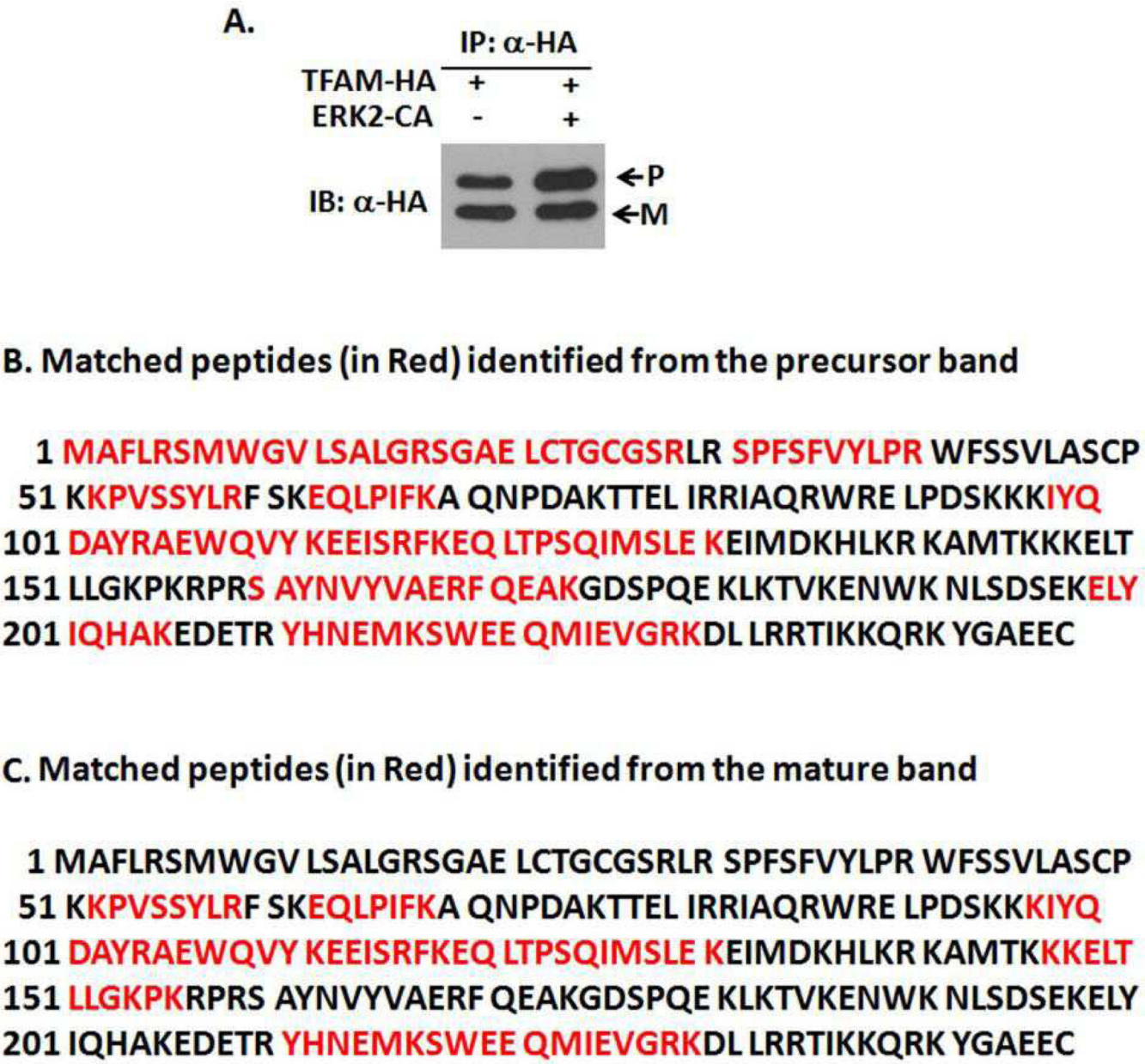

Fig. 2.

Protein ID of TFAM-HA verified by mass spectrometry. The TFAM-HA plasmid was either overexpressed alone or co-expressed with an ERK2-CA plasmid in SH-SY5Y cells for 48 h. Recombinant TFAM was then immunoprecipitated using anti-HA conjugated magnetic beads. Each eluted protein sample was split for loading in parallel lanes on the same 12% SDS-gel, with one lane loaded with 90% and the other loaded with 10% of the total eluate. (A) After electrophoresis, the gel piece containing 10% of the eluted proteins was transferred to a PVDF membrane and immunoblotted for HA. (B & C) The gel piece loaded with 90% of the eluted proteins was stained with Coomassie blue. The precursor and mature TFAM-HA bands (corresponding to the HA-Tag immunoreactive bands in (A)) were excised for trypsin in-gel digestion, and analyzed using MALDI-TOF/TOF. The matched

tryptic peptides of TFAM (UniprotKB/Swiss-Prot access number Q00059) are indicated in red characters.

A

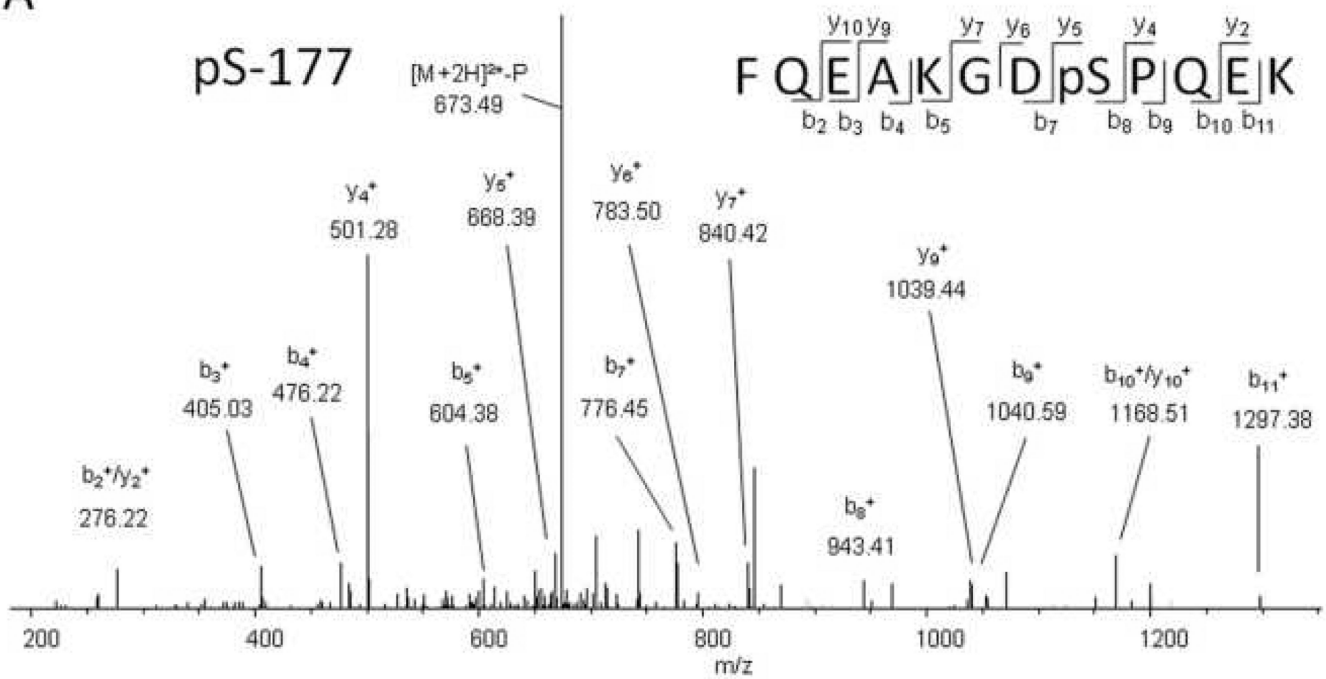

B

Phosphorylated residue	Sequence	pRS Probability	pRS Site Probabilities	Modifications
S-177	FQEAKGDsPQEK	1	S(8): 100.0	S8(Phospho)

Fig. 3.

Identification of ERK-directed phosphorylation sites of TFAM in cells. TFAM-HA was co-expressed with either a control plasmid or with a constitutively active ERK2 plasmid (ERK2-CA) in SH-SY5Y cells for 48 h, followed by immunoprecipiration of TFAM-HA. Eluted proteins were resolved by 4–15% SDS-PAGE and tryptic peptides generated by in-gel digestion. (A) MS/MS spectra of ERK2-dependent TFAM phosphopeptides modified at S-177 from the TFAMHA and ERK2-CA co-expressed sample. Peptide sequences were identified using the SEQUEST algorithm. (B) The phosphorylation sites were localized using the PhosphoRS algorithm and site probabilities >90% were considered high confidence. Phosphorylated Residue: Position of phosphorylated Serine (S) or Threonine (T) in TFAM (Q00059); Sequence: amino acid sequence of tryptic peptides with the phosphorylated residue displayed in lowercase; pRS probability: probability that the isoform is correct with a maximum value of 1; pRS Site Probabilities: Percent probability for each possible phosphorylation site on the peptide. Modifications: amino acid residue, position, and type of modification on the peptide.

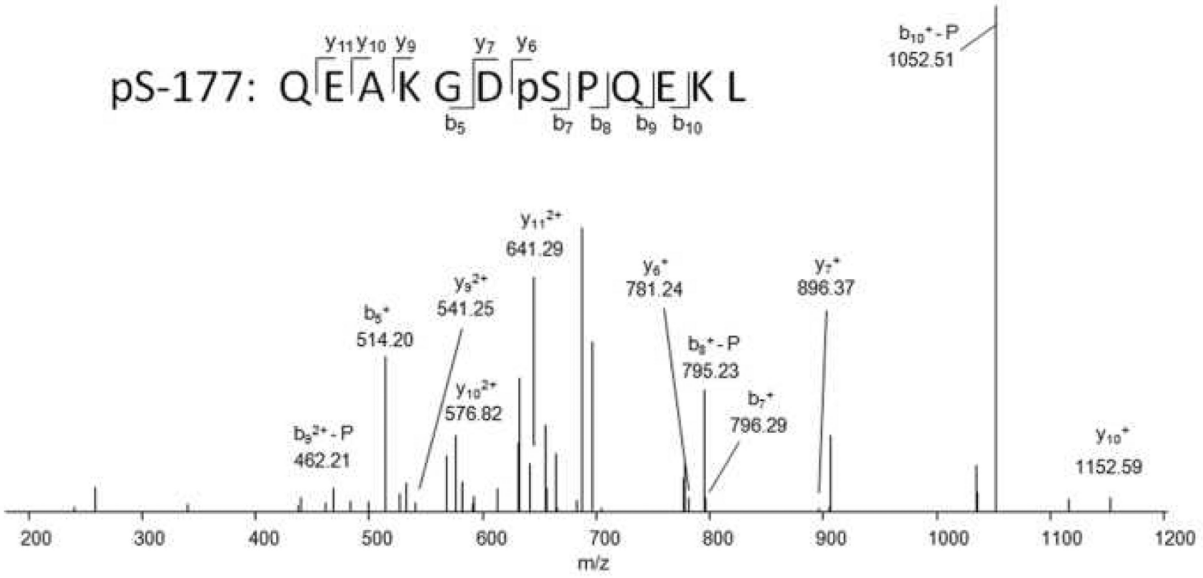

Phosphorylated residue	Sequence	pRS Probability	pRS Site Probabilities	Modifications
S-177	QEAKGDsPQEKL	1.0	S(7): 100.0	S7(Phospho)

Fig. 4.

Identification of *in vitro* ERK2-mediated phosphorylation of TFAM. (A) TFAM *in vitro* phosphorylation reaction was carried out as described in the Materials and Methods. After the reaction, proteins were loaded into a 4–15% SDS polyacryamide gel as: 90% of the reaction to one lane and another 10% of the reaction to a separate lane. After electrophoresis, the gel was sliced into two pieces. The gel piece loaded with 90% of the proteins was stained with Coomassie blue G250. The major protein bands (50 and 38 kD) were excised for trypsinization and MS analysis. Proteins from the other gel piece were transferred onto a PVDF membrane and immunoblotted with anti-TFAM and anti-ERK1/2. (B) Tryptic peptides prepared from the 50 and 38 KD protein bands were analyzed by MALDI-TOF/TOF-MS. All identified peptide fragments are highlighted in red. (C) Chymotryptic peptides from the 50 KD band (full-length GST-TFAM) were analyzed by LC-MS/MS and phosphorylation at (S177) of TFAM was identified.

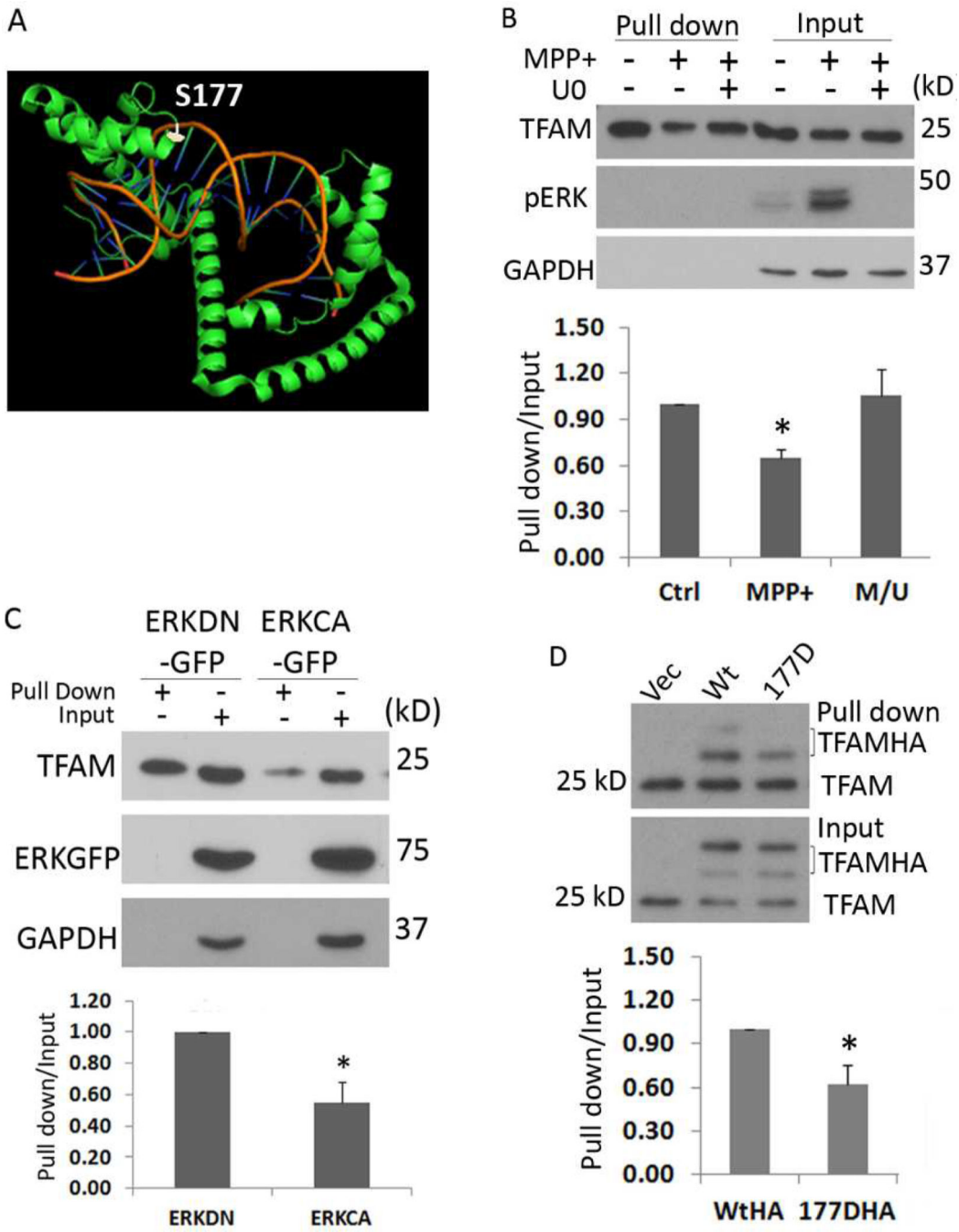

Fig. 5.

TFAM binding to LSP is reduced by ERK-mediated phosphorylation at S177. (A) The 3D structure of the TFAM-LSP DNA complex (RSCB: 3TMM) rendered with PyMOL predicts that residue S177 (white) is bound to the minor groove of the LSP DNA. (B) RA differentiated SH-SY5Y cells were treated with the indicated reagents for 6 days. Endogenous TFAM protein from each cell lysate was pulled down with a biotinylated DNA probe derived from the mitochondrial D-loop region (biotin-LSP) and analyzed by Western Blot. (C) Endogenous TFAM binding to the LSP was analyzed in HEK 293 cells transfected

48 h prior with plasmids encoding dominant negative ERK2-GFP (ERK2DN-GFP or ERKDN) or constitutively activated ERK2-GFP (ERK2CA-GFP or ERKCA). (D) The indicated TFAM-HA and mutant plasmids were transfected into HEK 293 cells for 48 h. Biotin-LSP + streptavidin-magnetic beads were used to pull-down TFAM for detection using anti-TFAM antibody. Note reduced pull-down of the 177D mutant despite equivalent expression in the input, and equivalent pull-down of endogenous (wild-type) TFAM (bottom bands in the pull-down) serves as an internal control. The relative TFAM-LSP binding shown in (B–D) was calculated as the ratio of the TFAM band from the pull down normalized to input, and presented as Mean ± SEM of three independent experiments. Asterisks indicate $p<0.05$ (MPP+ versus vehicle control in B; ERKCA versus ERKDN in C; 177DHA versus WtHA in D).

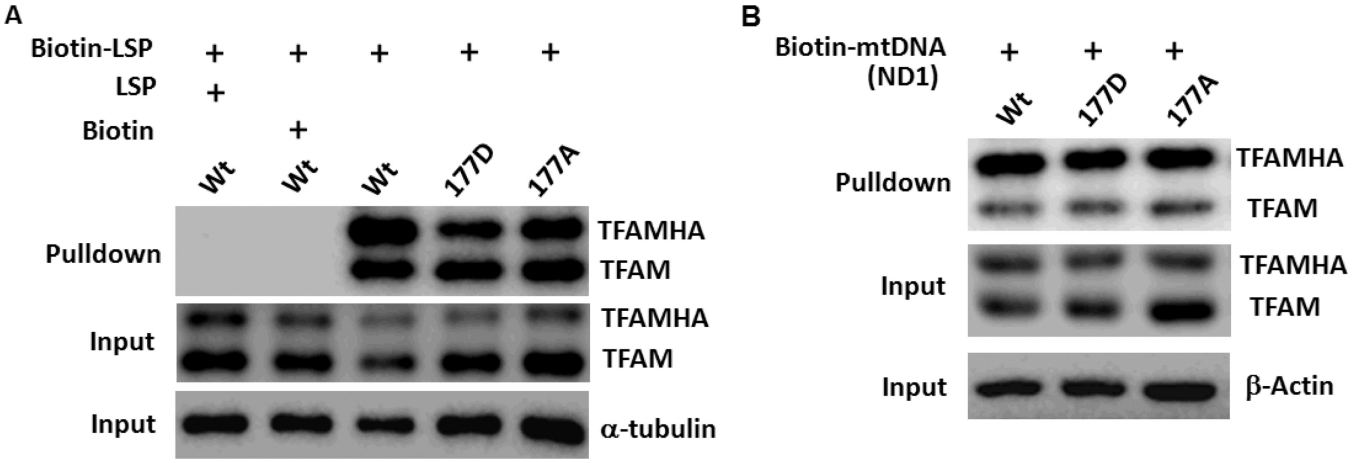

Fig.6.

Relative binding of TFAM mutants to LSP and non-specific mtDNA. HEK 293 cells were transfected with TFAM-HA, TFAM(S177D)-HA and TFAM(S177A)-HA mutant plasmids for 48 h and lysed for further analysis. (A) Biotin-LSP and streptavidin-magnetic beads were used to pull-down TFAM for detection using anti-TFAM antibody similar to the procedure shown in Fig. 5D. To validate the LSP binding specificity to TFAM, either 10 times (molar ratio) of non-labeled LSP or free biotin was pre-incubated with an equal amount of lysate containing wildtype TFAM and streptavidin-magnetic beads for 2 h prior to addition of the biotin-LSP probe. (B) A biotinylated mtDNA probe (biotin-mtDNA) derived from a coding region of the *Homo sapiens* ND1 was used to pull-down TFAM from cell lysates transfected with TFAM-HA, TFAM(S177D)-HA or TFAM(S177A)-HA. There were no differences in the non-specific mtDNA binding of the tested mutants relative to wild-type TFAM-HA. Representative data from 2 independent experiments is shown. Symbol designations in figure panels: Wt as TFAM-HA, 177D as TFAM(S177D)-HA and 177A as TFAM(S177A)-HA.

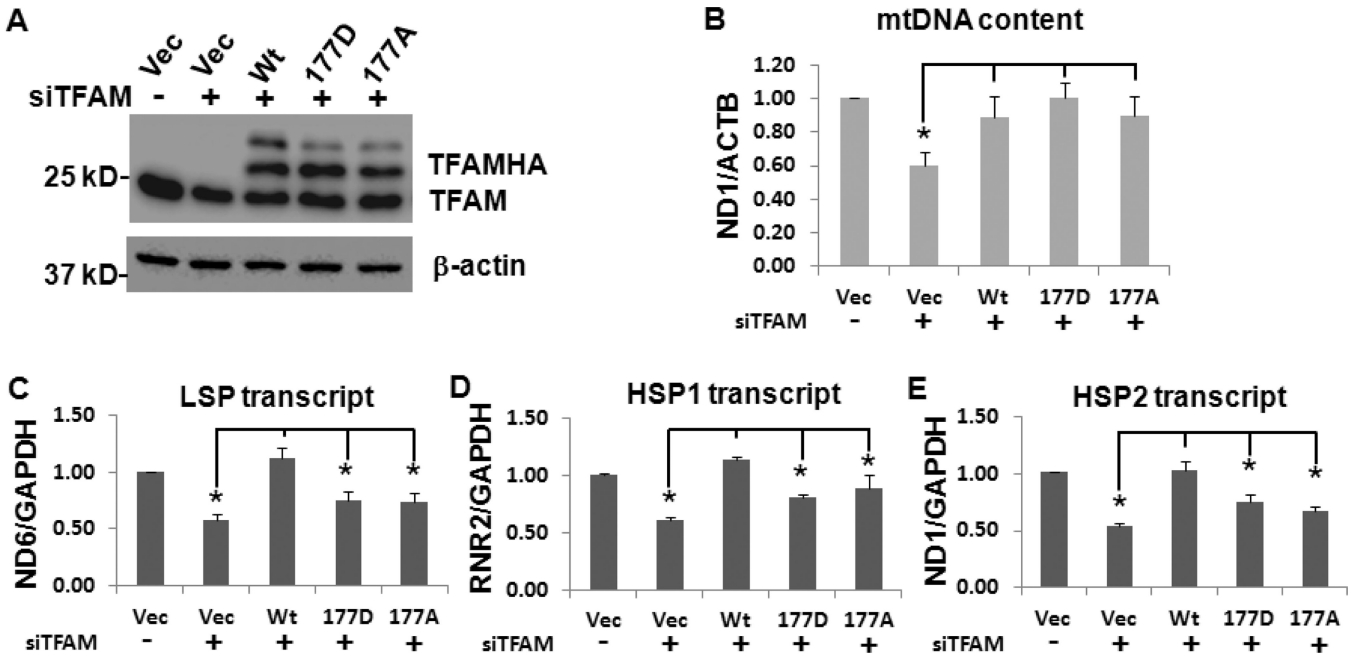

Fig. 7.

TFAM(177D)-HA is incapable of rescuing mitochondrial transcription incurred by knockdown of endogenous TFAM. HEK293 cells were first transfected with siCtrl or siTFAM for 24 h to knockdown endogenous TFAM, followed by transfection of TFAM-HA plasmids or control vector for another 48 h. (A) The expression levels of the endogenous TFAM and TFAM-HA wild-type and mutant proteins were analyzed by western blot. (B) mtDNA content analyzed by qPCR for ND1 normalized to ACTB. (C-D) The steady-state levels of mitochondrial transcripts of the light strand promoter (LSP), heavy strand promoter 1 (HSP1), and heavy strand promoter 2 (HSP2) were analyzed by qRT-PCR. Data presented in B-E were averaged from five independent experiments and represented as mean ± SEM. Asterisks indicate $p<0.05$ compared with the Wt. Symbols presented in figure panels: Vec as vector control, Wt as TFAM-HA, 177D as TFAM(S177D)-HA and 177A as TFAM(S177A)-HA.

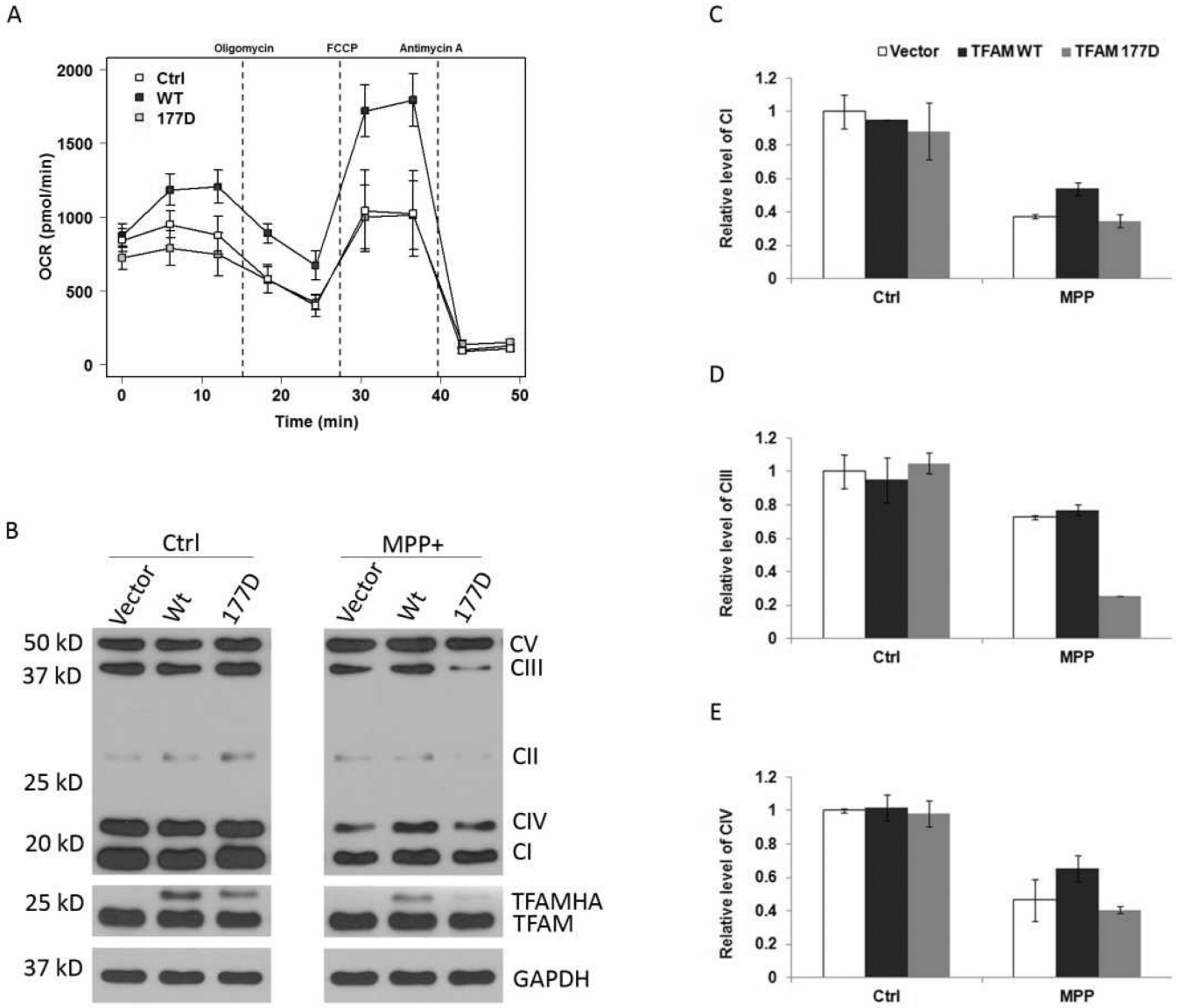

Fig. 8.

Effects of phosphomimetic TFAM mutations on mitochondrial respiration and respiratory protein levels. (A) Mitochondrial respiration of HEK293 cells transfected with the indicated forms of TFAM was analyzed by measuring the oxygen consumption rate (OCR) in a Seahorse XF24 extracellular flux analyzer. (B) SHSY5Y cells were transfected with either a control vector or the indicated TFAM plasmid for 24 h followed by MPP+ (2.5 mM) for another 24h. Mitochondrial respiratory protein content was analyzed by western blot using an OXPHOS antibody cocktail that detects one protein from each of respiratory complexes I to V. (C–E) Quantification of complex I, III and IV proteins in transfected cells with vehicle or MPP+ treatment, and normalized to GAPDH. Data were averaged from two independent experiments; error bars indicate the range.